Paraelectric–Ferroelectric Transition in the Lamellar Thiophosphate $CuInP_2S_6$

A. Simon and J. Ravez

Laboratoire de Chimie du Solide du CNRS, Université de Bordeaux I, 351 cours de la Libération, 33405 Talence Cedex, France

V. Maisonneuve, C. Payen, and V. B. Cajipe*

Institut des Matériaux de Nantes, CNRS-UMR 110, 2, rue de la Houssinière, 44072 Nantes Cedex 03, France

Received February 28, 1994. Revised Manuscript Received May 22, 1994®

The occurrence of a first-order paraelectric–ferroelectric phase transition at $T_C = 315(5)$ K in $CuInP_2S_6$ is revealed by calorimetry, X-ray powder diffraction, and dielectric measurements. This is the first observation of such a phenomenon in a thiophosphate of the lamellar MPS_3 family. The data are consistent with the polar character of the room-temperature structure attributable to the acentric positions of the Cu^I and In^{III} ions and may be related to the probable T dependence of the site-occupation ratios for the former cation and displacement of the latter. Results of the dielectric measurements are suggestive of a two-component phase transition.

Introduction

With the synthesis of phases derived by heterocharge substitution for the divalent cation M in lamellar MPS_3,[1] interest in this family of thiophosphates has shifted from the properties traditionally associated with a layered morphology to the novel structural and physical characteristics of the two different cationic sublattices thus formed.

The principal substituted compounds $M^IM'^{III}P_2S_6$[2-7] and $M^I_2M'^{II}P_2S_6$,[8,9] where M^I = Ag, Cu, M'^{II} = Mn, Zn and M'^{III} = Cr, V, In, Sc, consist of $[SM_{1/3}M'_{1/3}(P_2)_{1/3}S]$ or $[SM_{2/3}M'_{1/3}(P_2)_{1/3}S]$ layers in which the cations and P–P pairs fill the octahedral holes defined by the sulfur framework. A good example of the coloring problem[5] is encountered in the $a-b$ plane of the layer with the appearance of either zigzag chains or next-nearest-neighbor triangles of M and M′. Magnetic phenomena due to the low-dimensional arrangements of moment-carrying M'^{III}[2-4] have been extensively investigated, notably in $AgVP_2S_6$ and $AgCrP_2S_6$ which have provided excellent model systems for the study of quasi-one-dimensional Heisenberg antiferromagnetism.[10] Work focusing on the other cation, M^I, has been motivated by the presence of an extended electronic density around its central octahedral site; this feature has until now been explored from a predominantly structural viewpoint.[11-14]

The $CuM'P_2S_6$ (M'^{III} = Cr, V) phases are most illustrative of the various questions and possibilities raised by the occurrence of smeared electronic or nuclear densities in these materials. At room temperature (RT) for both compounds, difference Fourier maps calculated to locate the Cu^I within its octahedron reveal an electronic density continuum perpendicular to the layer.[2,6] Three types of vertically disposed and partially filled "split" positions with large anisotropic thermal factors have been employed to model the copper distribution: a distinctly off-center Cu1, a nearly central or octahedral Cu2, and a third tetrahedral Cu3 in the van der Waals (vdW) gap between the layers (see Figure 1, top). A 2-fold axis along b in the two RT structures leads to twice as many possible positions per copper octahedron. In $CuVP_2S_6$ all three positions are occupied with respective ratios of 0.53, 0.278, and 0.132 per octahedron,[6] while in $CuCrP_2S_6$ only the first two are filled with 0.66 and 0.34 occupation ratios.[2]

Low-temperature (LT) neutron powder diffraction studies have further differentiated these compounds vis-à-vis the behavior of the copper ions. On one hand, a repartitioning of the cations between two equivalent

* To whom correspondence should be addressed.

® Abstract published in *Advance ACS Abstracts,* July 1, 1994.

(1) Brec, R. *Solid State Ionics* **1986**, *22*, 3.
(2) Colombet, P.; Leblanc, A.; Danot, M.; Rouxel, J. *J. Solid State Chem.* **1982**, *41*, 174.
(3) Colombet, P.; Leblanc, A.; Danot, M.; Rouxel, J. *Nouv. J. Chim.* **1983**, *7*, 333.
(4) Lee, S.; Colombet, P.; Ouvrard, G.; Brec, R. *Mater. Res. Bull.* **1986**, *21*, 917.
(5) Lee, S. *J. Am. Chem. Soc.* **1988**, *110*, 8000 and references therein.
(6) Durand, E.; Ouvrard, G.; Evain, M.; Brec, R. *Inorg. Chem.* **1990**, *29*, 4916.
(7) Maisonneuve, V.; Evain, M.; Payen, C.; Cajipe, V. B.; Molinié, P. *J. Alloys Compounds*, in press.
(8) Mathey, Y.; Clement, R.; Audiere, J. P.; Poizat, O.; Sourisseau, C. *Solid State Ionics* **1983**, *9–10*, 459.
(9) (a) Evain, M.; Boucher, F.; Brec, R.; Mathey, Y. *J. Solid State Chem.* **1991**, *90*, 8. (b) Boucher, F.; Evain, M.; Brec, R. *Eur. J. Solid State Inorg. Chem.* **1991**, *28*, 383.
(10) (a) Mutka, H.; Payen, C.; Molinié, P.; Soubeyroux, J. L.; Colombet, P.; Taylor, A. D. *Phys. Rev. Lett.* **1991**, *67*, 497 and references therein. (b) Mutka, H.; Payen, C.; Molinié, P. *Europhys. Lett.* **1993**, *21*, 623.
(11) Van Der Lee, A.; Boucher, F.; Evain, M.; Brec, R. *Z. Kristallogr.* **1993**, *203*, 247.
(12) Burr, G. L.; Durand, E.; Evain, M.; Brec, R. *J. Solid State Chem.* **1993**, *103*, 514.
(13) Maisonneuve, V.; Cajipe, V. B.; Payen, C. *Chem. Mater.* **1993**, *5*, 758.
(14) (a) Mathey, Y.; Mercier, H.; Michalowicz, A.; Toffoli, P.; Leblanc, A. *J. Phys. Chem. Solids* **1985**, *46*, 1025. (b) Poizat, O.; Sourisseau, C. *J. Solid State Chem.* **1985**, *59*, 371. (c) Payen, C.; McMillan, P.; Colombet, P. *Eur. J. Solid State Inorg. Chem.* **1990**, *27*, 881.

0897-4756/94/2806-1575$04.50/0

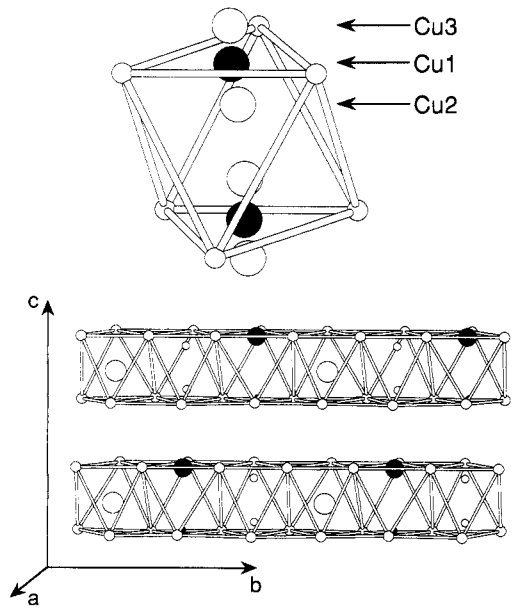

Figure 1. (top) Sulfur octahedral cage showing the various types of copper sites, namely, the off-center Cu1, the nearly central Cu2, and the tetrahedral Cu3 in the vdW gap. The two off-center sites become inequivalent when unequally occupied, leading to the appearance of the distinguishable $Cu1^u$ (up) and $Cu1^d$ (down) positions. (bottom) Two layers of $CuInP_2S_6$ separated by the vdW gap.[7] At room temperature (RT) the Cu^I are predominantly in the upper off-center $Cu1^u$ site and the In^{III} is slightly displaced downward from the octahedral center. The RT monoclinic lattice parameters[7] are a = 6.0956(4) Å, b = 10.5645(6) Å, c = 13.6230(8) Å and β = 107.101(3)°; the perpendicular to the layers is the c^* axis which is about 17° forward of the plane of the page.

Cu1 sites per octahedron, i.e., an emptying of the Cu2 and Cu3, was observed in $CuVP_2S_6$ at 20 K.[12] On the other, the formation of an antipolar copper sublattice was reported in $CuCrP_2S_6$ below 150 K:[13] an array of alternating dipoles appears with the complete occupation of inequivalent $Cu1^u$ (up) and $Cu1^d$ (down) sites related by a ($^1/_2$,$^1/_2$,0) translation. While both results favor a thermal hopping over a spatial disorder interpretation[13] of the RT copper distribution in these phases, the second experiment moreover ruled out the debated existence of Cu–Cu pairs[6,13,14] in $CuM'P_2S_6$.

The prospects for unusual properties associated with a $CuM'P_2S_6$ composition intensified very recently with the determination of the crystal structure of $CuInP_2S_6$.[7] This compound has a practically polar copper sublattice at room temperature: the Cu^I ions occupy inequivalent $Cu1^u$ and $Cu1^d$ sites, each off center by about 1.58 Å and with respective ratios of 0.875–0.100 per octahedron so that the RT structure is noncentrosymmetric with space group *Cc* (see Figure 1, bottom). Note that in the thermal hopping model, this copper distribution would correspond to an incipient freezing of the motion between two potential minima of unequal depths.[7] Furthermore, the In^{III} was found to be displaced ≈0.2 Å downward from the center of its octahedron following the preponderant occupation of the upper $Cu1^u$ site. It is obvious from these features that, first, a phase transition involving a loss of polarity should exist in this compound at a temperature not very different from ambient, and second, interesting T-dependent dielectric behavior accompanying the structural transformation may be expected.

In this paper, we present calorimetry, X-ray powder diffraction, and more importantly dielectric measurement evidence for the occurrence of a first-order paraelectric–ferroelectric transition at T_C = 315(5) K in $CuInP_2S_6$. The data from the last-mentioned technique represent the first investigation of the dielectric properties of a lamellar MPS_3-type phase. Structurally and chemically, $CuInP_2S_6$ is significantly different from the well-studied ferroelectric, $Sn_2P_2S_6$, in which the $(P_2S_6)^{-4}$ anions are linked together by S–Sn contacts to yield a three-dimensional connectivity, and which exhibits a second-order, predominantly displacive transition at around 333 K.[15] It may then be said that the results described here mark the discovery of a new class of layered thiophosphate ferroelectric materials.

Experimental Section

$CuInP_2S_6$ was prepared as previously described[7] in both powder and crystal form; samples were analyzed via EDS with a scanning electron microscope. Differential scanning calorimetry (DSC) measurements were made on ≈60 mg powder samples under nitrogen using a Perkin-Elmer DSC-4 apparatus calibrated with cyclohexane (melting point at T = 279.69K with ΔH = 7.47 cal/g); temperature cycling was done at 10 K/min.

X-ray powder diffraction patterns were obtained with a Siemens D5000 diffractometer in a Bragg–Brentano configuration employing Ni-filtered Cu Kα radiation and a $Na_2Ca_3Al_2F_{14}$-calibrated linear detector subtending a 6° angle. To carry out temperature-dependent studies, the diffractometer was equipped with an evacuated chamber with a kapton window and a flat-plate sample mount cooled by a flow of liquid nitrogen and heated by an appropriate resistance; the temperature was regulated and measured to an accuracy of ±1°. The unit-cell parameters at different temperatures were extracted by performing full-profile fits on the corresponding diffraction patterns.[16]

Dielectric measurements were performed under dry nitrogen at temperatures between 290 and 360 K, using a Wayne-Kerr 6425 automatic component analyzer operating in a 20 Hz–

(15) According to: (a) Scott, B.; Presspich, M.; Willet, R. D.; Cleary, A. *J. Solid State Chem.* **1992**, *96*, 294, the Sn^{2+} ions move by 0.22 or 0.35 Å, mainly along the (100) direction in $Sn_2P_2S_6$ as the ferro–paraelectric transition occurs. There is strong evidence that this phase transition is predominantly displacive. Low-frequency modes which soften at the transition occur in this compound and have been extensively studied. See for example: (b) Vysochanskii, Yu. M.; Slivka, V. Yu.; Buturlakin, A. P.; Gurzan, M. I.; Chepur, D. V. *Sov. Phys. Solid State* **1978**, *20(1)*, 49. (c) Vysochanskii, Yu. M.; Slivka, V. Yu.; Voroshilov, Yu. V.; Gurzan, M. I.; Chepur, D. V. *Sov. Phys. Solid State* **1979**, *21(8)*, 1382. (d) Volkov, A. A.; Kozlov, G. V.; Afanas'eva, N. I.; Vysochanskii, Yu. M.; Grabar, A. A.; Slivka, V. Yu. *Sov. Phys. Solid State* **1983**, *25(9)*, 1482. (e) Grabar, A. A.; Vysochanskii, Yu. M.; Slivka, V. Yu. *Sov. Phys. Solid State* **1984**, *26(10)*, 1859. A microwave study showed that the soft ferroelectric mode is overdamped, i.e., transforms into a relaxational one close to the transition, implying an order-disorder contribution to the dynamics; see: (f) Grigas, J.; Kalesinskas, V.; Lapinskas, S.; Gurzan, M. I. *Phase Transitions* **1988**, *12*, 263. Such overdamping has also been observed in $BaTiO_3$ which is nevertheless, like $Sn_2P_2S_6$, still referred to as a displacive ferroelectric; see: (g) Lines, M. E.; Glass, A. M. *Principles and Applications of Ferroelectrics and Related Materials*; Clarendon Press: Oxford, 1979; pp 241–246. Note that $Sn_2P_2S_6$ has a Curie–Weiss constant comparable to those of the predominantly displacive ferroelectric perovskites; see: (h) Maior M. M., Bovtun, V. P., Poplavko, Yu. M., Koperles, B. M.; Gurzan, M. I. *Sov. Phys. Solid State* **1984**, *26(3)*, 397. The general consensus is that the phase transition in $Sn_2P_2S_6$ is second order. Some recent publications on $Sn_2P_2S_6$ and related materials are: (i) Slivka, A. G.; Gerzanich, E. I.; Guranich, P. P.; Shusta, V. S. *Ferroelectrics* **1990**, *103*, 71. (j) Arnautova, E.; Sviridov, E.; Rogach, E.; Savchenko, E.; Grekov, A. *Integrated Ferroelectrics* **1992**, *1*, 147. (k) Cleary, D.A.; Willett, R. D.; Ghebremichael, F.; Kuzyk, M. G. *Solid State Commun.* **1993**, *88*, 39. (l) Apperley, D. C.; Harris, R. K.; Cleary, D. A. *Chem. Mater.* **1993**, *5*, 1772.

(16) Murray, A. D.; Fitch, A. N. *MPROF, A Multipattern Rietveld Refinement Program for Neutron, X-ray and Synchrotron Radiation*, 1989.

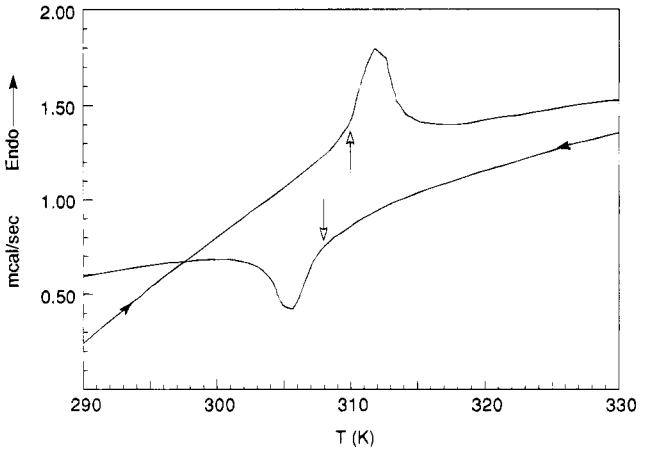

Figure 2. Warming and cooling differential scanning calorimetry thermograms of a 66 mg powder sample of $CuInP_2S_6$; the vertical white arrowheads indicate the onset temperatures for each cycle.

300 kHz frequency range. For these, crystal samples approximately 10 mm^2 in area and 16 μm thick were used. Gold electrodes were deposited on the flat faces of each sample across which an electric field of about 625 V/cm was applied; measurements were thus made perpendicular to the layers (see Figure 1b). The heating/cooling rate was 1.5 K/min.

Results and Discussion

Calorimetry. Evidence for a phase transition in $CuInP_2S_6$ was first given by DSC measurements made on powder samples. An endothermic peak was observed during a warming scan (Figure 2) with an onset temperature of 310(1) K and energy $\Delta H = 0.10(1)$ cal/g. Upon cooling, the transition shifts to a slightly lower $T = 308(1)$ K. Cycling the standard cyclohexane through its melting point under similar conditions reveals a thermal hysteresis of the same magnitude, i.e., 280(1) K versus 278(1) K. Moreover, the temperature widths of the sample and cyclohexane thermogram peaks were both found to be about 2 K. The $CuInP_2S_6$ transition thus appears to be as narrow and weakly hysteretic as the fusion of the calibrating standard.

X-ray Powder Diffraction. A preliminary study of the transition at 310 K was subsequently undertaken by monitoring the lattice parameters and the relative powder diffraction peak intensities as a function of temperature.

The evolution of a, b, c, β, and the cell volume V with heating is traced in Figure 3; these results coincide within experimental error with those from a cooling cycle (not shown). It is clear from these curves that the $CuInP_2S_6$ cell dimensions increase much more rapidly between 273 and 350 K than elsewhere on the temperature axis; the inflection point for the lattice lengths is at T = 310 K. An average coefficient of volume expansion $\alpha_V = \Delta V/(V_0 \Delta T)$, where V_0 is the room temperature volume, $\Delta T = T - 293$ K and $\Delta V = V - V_0$, may be calculated to yield a maximum around T = 310 K (inset to middle frame of Figure 3). As might be expected from the compound's morphology, the thermal expansion is up to 3 times larger along c than in the plane of the layers. The degree of anisotropy is conserved as the dilation induced by the transition occurs. This anomalous volume increase however spans a much wider temperature range than inferred from the DSC data, suggesting that the structural transformation

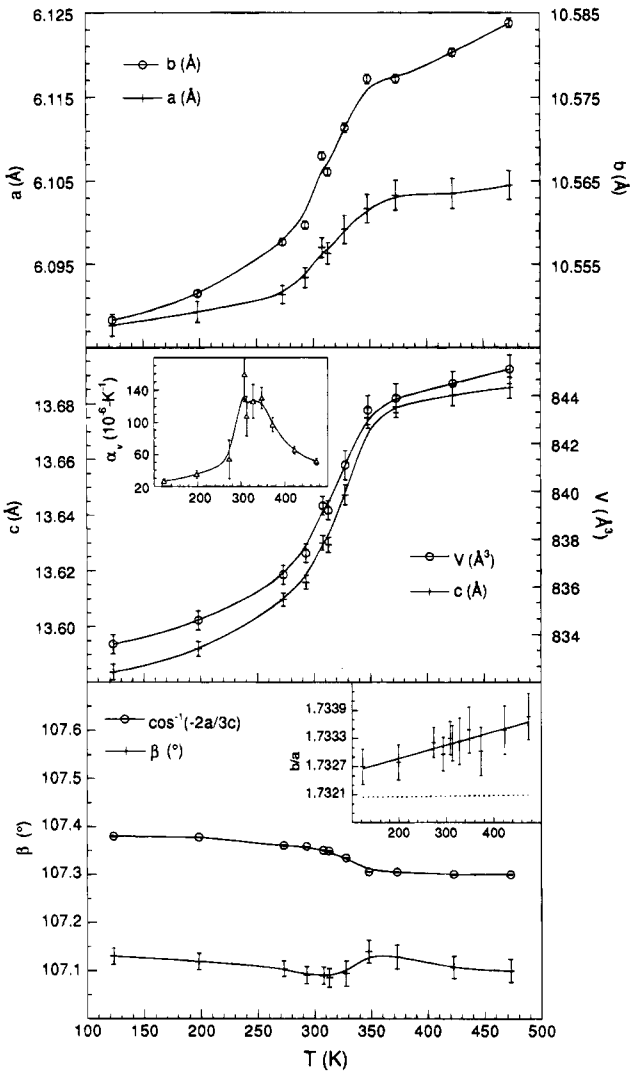

Figure 3. Evolution of the lattice parameters a, b, c, β, and V of $CuInP_2S_6$ with temperature. Middle panel inset: variation of the average coefficient of volume expansion $\alpha_V = \Delta V/(V_0 \Delta T)$, where V_0 is the room-temperature volume, $\Delta T = T - 293$ K and $\Delta V = V - V_0$. Bottom panel: the upper curve is $\cos^{-1}(-2a/3c)$ to be compared with the lower β plot, while the inset shows b/a values greater than $\sqrt{3}$ marked by the dashed line.

involves more than the single thermal event measured by calorimetry.

Chalcogen stacking distortions are known to arise in the substituted MPS_3 phases as a consequence of the unequal cation sizes.[17] These have been described in terms of the deviations of b/a and β from their respective ideal values $\sqrt{3}$ and $\cos^{-1}(a/3c_0)$, where c_0 is the interlayer distance, equal to $c/2$ in the present case: the first quantity characterizes in-plane and the second, out-of-plane packing deformations. The bottom panel of Figure 3 shows that b/a becomes increasingly larger than $\sqrt{3}$ as T is raised, while the difference between β and $\cos^{-1}(2a/3c)$ decreases above 310 K. Similar tendencies with heating have been noticed in the related compound $Ag_2MnP_2S_6$.[11] The enhanced planar distortions therein were attributed to the distribution of the Ag^I ion over more sites, including the tetrahedral ones in the vdW gap, at high T; the filling of these latter in

(17) Ouvrard, G.; Brec, R. *Eur. J. Solid State Inorg. Chem.* **1990**, *27*, 477.

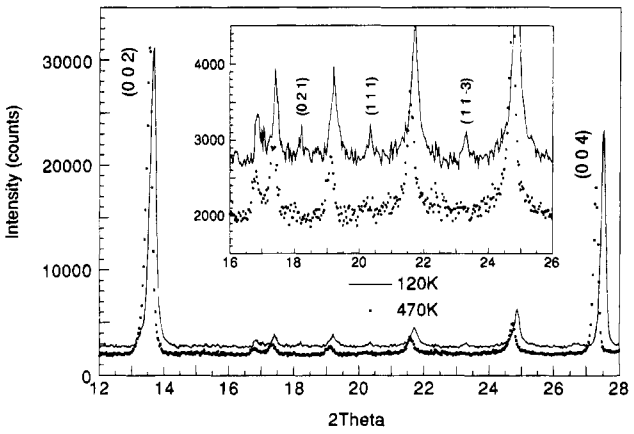

Figure 4. Comparison of part of the X-ray powder diffraction pattern of $CuInP_2S_6$ at 120 K (top) and 470 K (bottom) showing the cooling-enhanced (021), (111), and (11−3) intensities and (004) to (002) intensity ratio.

turn leads to strengthened interlayer bonding, i.e., reduced interplanar distortions. Assuming this interpretation to be correct, it would appear that raising T above the transition temperature in $CuInP_2S_6$ likewise induces the occupation of all three Cu1-, Cu2-, and Cu3-type sites, each of which exists in pairs within a copper octahedron. On the other hand, the quantities b/a and β conceal local effects such as the swelling of the upper S-triangles of the CuS_6 units and the concurrent twisting of the PS_3 groups and In octahedra observed at RT:[7] along with the copper distribution, these strains should certainly evolve with temperature and influence the lattice parameters.

Additional insight into the transition mechanism may be obtained by comparing the relative intensities of certain reflections at different temperatures. The (021), (111), and (11−3) peaks, which are weak but very visible below 310 K, are observed to lose intensity at higher T and are no longer detectible when $T > 328$ K (see Figure 4 inset). Powder pattern simulations show that these reflections are appreciably stronger in a $CuInP_2S_6$ structure with a completely polar Cu sublattice (100% occupation of upper $Cu1^u$ site) than in one where the Cu equally occupies two off-center sites straddling its octahedral center (see Figure 1, top). The (004) to (002) intensity ratio was also smaller in the pattern calculated for the nonpolar case and found to diminish further with the introduction of partially filled Cu2 and/or Cu3 sites. As Figure 4 demonstrates, such a $I(004)/I(002)$ ratio decrease indeed occurs with increased temperature.

To summarize, the powder diffraction data suggest that, in a heating cycle, the transition involves an anomalous volume increase accompanying a more fundamental polar to nonpolar change in symmetry of the structure (*Cc* to *C*2/*c*). This change is most likely brought about by the temperature variation of the occupation ratios of the different Cu^I sites and the concomitant In^{III} displacement. Whereas the expansion between 273 and 350 K conceivably reflect gradual structural rearrangements associated with changing copper site occupancies or motions, the loss of polarity itself probably occurs abruptly around 310 K as indicated by DSC. The rapid volume increase thereafter until 350 K may be related to the Cu^I hopping into the vdW gap.

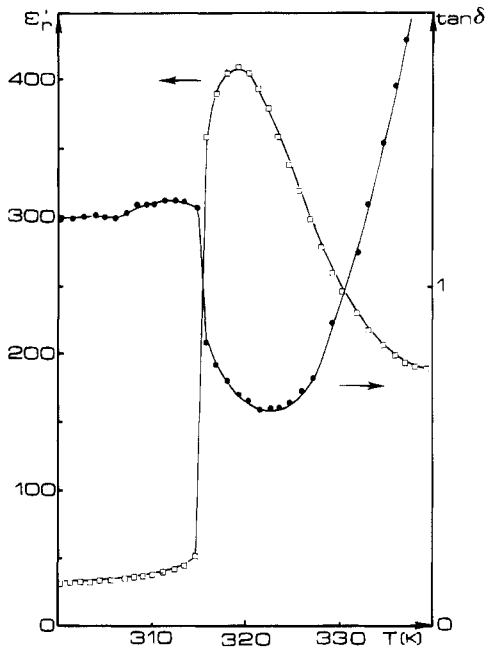

Figure 5. Temperature dependence of ϵ_r' and tan δ measured, perpendicular to the layers (along c^*), on a crystal sample during heating at 1 kHz.

Dielectric Measurements. Confirmation of the polar nature of the transition was then sought by performing dielectric measurements. Figure 5 shows the temperature dependence of both the real permittivity ϵ_r' and the tangent of the dielectric loss angle, tan δ, measured on a crystal at 1 kHz upon heating. The ϵ_r' maximum associated with a tan δ minimum is consistent with the occurrence of a ferroelectric-paraelectric phase transition at $T_C = 319(5)$ K, i.e., the disappearance with heating of the spontaneous polarization at this temperature. Since the electrodes were attached to the flat faces of the crystal sample, the effective polarization axis in these measurements lies along the perpendicular to the layers, i.e., the along c^* (see Figure 1, bottom).

Data obtained at various frequencies yield the $\epsilon_r' = f(T)$ curves of Figure 6, which imply a dielectric dispersion: the ϵ_r' maximum decreases from 410 to 190 as the frequency increases from 500 to 10^5 Hz. The temperature at which the dielectric anomaly occurs does not change with frequency, so $CuInP_2S_6$ behaves like a normal ferroelectric rather than a relaxor ferroelectric typified by the perovskite $PbMg_{1/3}Nb_{2/3}O_3$ (PMN).[18]

The shape of the dielectric peak, measured on warming as shown in Figures 5 and 6, is suggestive of a two-component phase transition: the steep rise of the permittivity at around 315 K is followed, not by a cusp as in $BaTiO_3$[19] or $NaNO_2$,[20] but by a somewhat round maximum. Note that the dielectric loss minimum has a similar round shape (Figure 5). Also, the tempera-

(18) In PMN, it has been suggested that the Mg and Nb ions do not order and thus Mg:Nb composition fluctuations exist leading to large fluctuations in the transition temperature and a mixture of polar and nonpolar micro regions over a wide temperature range. The temperature of the ϵ_r' maximum therein increases with frequency in a manner typical of a relaxation dielectric. See: Cross, L. E. *Ferroelectrics* **1987**, *76*, 241.

(19) Lines, M. E.; Glass, A. M. *Principles and Applications of Ferroelectrics and Related Materials*; Clarendon Press: Oxford, 1979; pp 133−141.

(20) In ref 19, p 327.

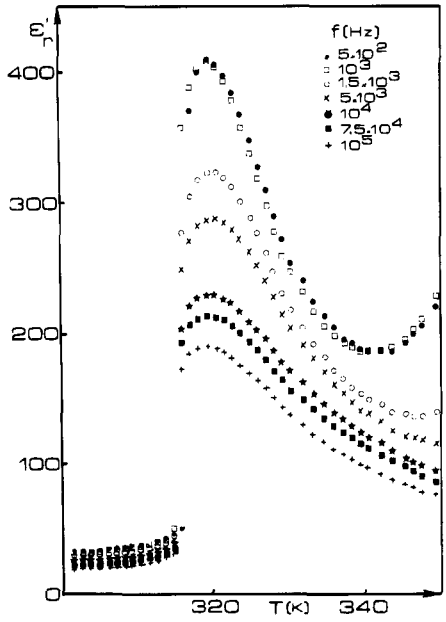

Figure 6. Real permittivity along c^* measured as a function of temperature, on a crystal and on heating, at various frequencies.

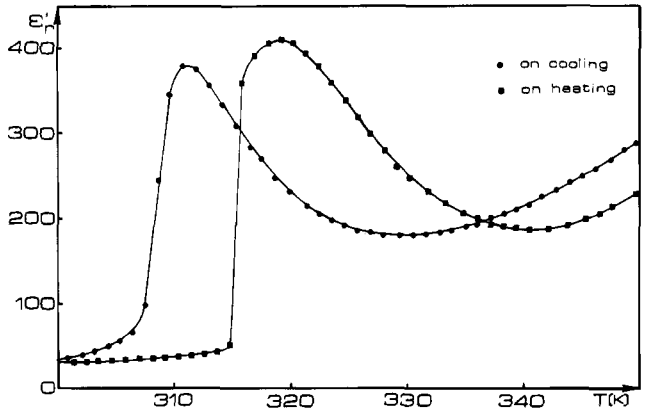

Figure 7. Thermal dependence of ϵ_r' on heating and cooling measured along c^* on a crystal at 1 kHz.

tures at which the ϵ_r' and tan δ extrema occur are not identical, implying that the transition is not perfectly sharp.[19] The spontaneous polarization in the ferroelectric phase may be attributed mainly to the Cu^I and In^{III} ions which have nonzero and antiparallel vertical offsets from their respective central octahedral sites at room temperature.[7] It is conceivable that the transition is very slightly broadened by the T dependence of the contributions of these cations to the polarization.

Notwithstanding the above observations, the transition in $CuInP_2S_6$ can be demonstrated to be of the first order. Figure 7 compares the behavior of the permittivity during a heating and cooling cycle; the maximum in the latter occurs at $T_C' = 311(5)$ K so that an 8 K wide thermal hysteresis is observed. Moreover, a Curie–Weiss law fit to the inverse permittivity $\epsilon_r'^{-1}$ in the paraelectric T range yields a Curie–Weiss temperature $T_0 = 299$ K, which is less than the transition temperature T_C' and thus likewise indicative of a first-order phase transition (Figure 8). Last, the ratio of the slope of the line through the $\epsilon_r'^{-1}$ data in the ferroelectric temperature range to that of the Curie–Weiss curve at higher T is very much greater than two, again as expected of transitions of first order.[19]

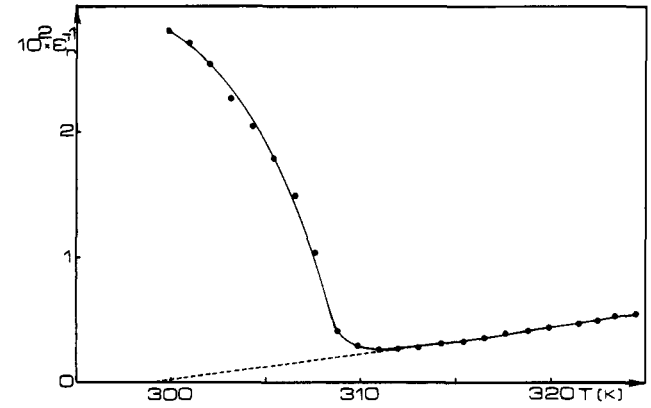

Figure 8. Inverse permittivity $\epsilon_r'^{-1}$ (dots) given for the cooling data of Figure 7, fitted with a Curie–Weiss law (solid line through data at $T > 310$ K extended with dashed line to lower T).

The Curie constant C calculated from Figure 8 is 4700 K. This is much smaller than those found in displacive ferroelectrics with oxygen octahedra, e.g., $C(BaTiO_3) = 1.6 \times 10^5$ K, and that in $Sn_2P_2S_6$ ($C \approx 10^5$ K)[15h] but is close to the values obtained for order–disorder ferroelectrics, e.g., $C(NaNO_2) = 5000$ K.[21] It would thus be tempting to say that $CuInP_2S_6$ is an order–disorder ferroelectric, especially since the assumed T dependence of the copper distribution in this compound lends itself easily to such an interpretation. However, the possibility of a displacive contribution from the indium ions cannot be dismissed.

The low frequency ($\leq 10^3$ Hz) data of Figure 6 also show that the permittivity increases above 340 K, signaling the probable occurrence of ionic conductivity at these temperatures. This hypothesis accords with the presence of Cu^I ions in the vdW gap at $T > 310$ K as inferred from the powder diffraction data. In addition, it would seem from Figure 7 that the temperature at which this conductivity is activated depends on the direction of the cycling: while the conductivity tail persists down to 330 K on the cooling curve, its rise upon warming is observed only after 340 K. Such a difference may be understood by considering that whereas the copper ions are presumably highly mobile before cooling from 350 K, their motions in the vdW gap are retarded by the requisite crossing of the basal triangles of the CuS_6 groups when heating from RT.

A final point to be addressed is the seeming discrepancy between the transition temperatures and thermal hysteresis widths indicated by DSC and the dielectric measurements. The calorimetry was done on a powder sample, i.e., an ensemble of small, conceivably single-domain crystallites, while the permittivity measurements were made on crystals which are most probably multidomain at RT. It is possible that relaxation effects associated with domain walls in a crystal slightly raises the transition temperature in a warming cycle. Heating the $CuInP_2S_6$ crystal sample yields a ϵ_r' maximum at 319(5) K which is fairly different from the DSC peak at 310(1) K, while cooling leads to an anomaly at 311(5) K which, within experimental error, overlaps with the DSC exothermic event at 308(1) K. The coincidence of

(21) Burfoot, J. C. *Ferroelectrics: An Introduction to the Physical Principles*, D. Van Nostrand: London, 1967; p 224.

the cooling cycle results is consistent with the absence of domains in the initial paraelectric state. On the other hand, it might be argued that calorimetry measures only the sharp component of the transition (ϵ_r' discontinuity at 315 K), i.e., is insensitive to the second one (ϵ_r' maximum at 319 K). In any case, the nonidentical measurement conditions may also be partly responsible for the temperature differences. All things considered, the Curie point may be given as $T_C = 315(5)$ K.

Conclusion

In this work, the occurrence of a first-order paraelectric–ferroelectric phase transition at $T_C = 315(5)$ K in $CuInP_2S_6$ was demonstrated using calorimetry, X-ray powder diffraction and dielectric measurement data. This is the first time that such a phenomenon has been observed in a thiophosphate of the extended lamellar MPS_3 family. The existence of a ferroelectric state is consistent with the polar character of the room structure in which Cu^{I} predominantly occupies an upper off-center position and the In^{III} is shifted downward from the midplane through the layer. Although the expectation of a temperature-dependent distribution of the copper over its possible sites implies an order–disorder transition, a displacive contribution from the indium is also conceivable.

We are presently investigating the structural aspects of this transition through detailed T-dependent X-ray studies on a single crystal. Also in progress are hysteresis loop, pyroelectric, piezoelectric and optical measurements which should reveal the magnitudes of various exploitable physical properties of this new ferroelectric (the spontaneous polarization, pyroelectric current, etc.). We are likewise studying the ionic conductivity associated with the supposed presence of copper in the vdW gap at high temperatures. Local probe experiments (high-resolution NMR, vibrational spectroscopies) are envisioned to test the thermal hopping model of the copper distribution, as well as confirm the displacive nature of the indium offset in this compound. Finally, it is obvious from the present results that the dielectric properties of the related $CuM'P_2X_6$ (X = S, Se) would be worthwhile investigating.

Acknowledgment. We wish to thank C. Gueho and S. Grolleau for their technical assistance during the diffraction and DSC measurements.